

The oral and gut microbiomes are perturbed in rheumatoid arthritis and partly normalized after treatment

Xuan Zhang^{1,13}, Dongya Zhang^{2,3,13}, Huijue Jia^{2,3,13}, Qiang Feng^{2,4,5,13}, Donghui Wang^{2,5,13}, Di Liang^{1,13}, Xiangni Wu¹, Junhua Li^{2,3,6}, Longqing Tang², Yin Li², Zhou Lan², Bing Chen², Yanli Li², Huanzi Zhong², Hailiang Xie², Zhuye Jie², Weineng Chen², Shanmei Tang², Xiaoqiang Xu^{2,7}, Xiaokai Wang^{2,7}, Xianghang Cai², Sheng Liu^{2,7}, Yan Xia^{2,7}, Jiyang Li^{2,8}, Xingye Qiao⁹, Jumana Yousuf Al-Aama^{2,10}, Hua Chen¹, Li Wang¹, Qing-jun Wu¹, Fengchun Zhang¹, Wenjie Zheng¹, Yongzhe Li¹, Mingrong Zhang², Guangwen Luo², Wenbin Xue², Liang Xiao^{2,3}, Jun Li², Wanting Chen², Xun Xu², Ye Yin², Huanming Yang², Jian Wang², Karsten Kristiansen^{2,5}, Liang Liu¹¹, Ting Li¹¹, Qingchun Huang¹², Yingrui Li² & Jun Wang^{2,5,11}

We carried out metagenomic shotgun sequencing and a metagenome-wide association study (MGWAS) of fecal, dental and salivary samples from a cohort of individuals with rheumatoid arthritis (RA) and healthy controls. Concordance was observed between the gut and oral microbiomes, suggesting overlap in the abundance and function of species at different body sites. Dysbiosis was detected in the gut and oral microbiomes of RA patients, but it was partially resolved after RA treatment. Alterations in the gut, dental or saliva microbiome distinguished individuals with RA from healthy controls, were correlated with clinical measures and could be used to stratify individuals on the basis of their response to therapy. In particular, *Haemophilus* spp. were depleted in individuals with RA at all three sites and negatively correlated with levels of serum autoantibodies, whereas *Lactobacillus salivarius* was over-represented in individuals with RA at all three sites and was present in increased amounts in cases of very active RA. Functionally, the redox environment, transport and metabolism of iron, sulfur, zinc and arginine were altered in the microbiota of individuals with RA. Molecular mimicry of human antigens related to RA was also detectable. Our results establish specific alterations in the gut and oral microbiomes in individuals with RA and suggest potential ways of using microbiome composition for prognosis and diagnosis.

RA is an autoimmune disorder affecting tens of millions of people worldwide and is associated with increased mortality owing to cardiovascular and other systemic complications. However, the etiology of RA remains elusive¹. Although studies on genetic predisposition to RA have implicated genes such as *HLA-DRB1*, *TNFAIP3*, *PTPN22* and *PADI4*, environmental factors have also been shown to contribute to disease pathogenesis^{1–5}. Microbial triggers have been implicated in RA¹; however, the identity and pathogenicity of specific microbes have remained unclear. Although there are reports of clinical success in reducing inflammation in RA with disease-modifying antirheumatic drugs (DMARDs), the development of specific and more effective therapies has been hindered by insufficient understanding of factors that trigger or promote the disease. Investigation of the microbiome might also reveal probiotics that could prevent or attenuate RA symptoms.

Although joint inflammation is characteristic of RA, inflammation may develop in other body sites years before the onset of joint inflammation^{1,6,7}. The gut microbiota is an environmental factor that influences metabolic and immune homeostasis^{8,9}. The composition of the gut microbiome is reasonably stable in a given individual^{10–12}; however, it is quite heterogeneous between individuals^{12,13}. The oral microbiome is relatively understudied compared with the gut microbiome, with the Human Microbiome Project sampling only healthy individuals for shotgun sequencing¹⁴. Metagenomic analysis of the oral microbiome and its association with disease has been lacking¹⁵, despite the fact that dental plaque and salivary samples are more readily obtained at clinical visits than fecal samples. It is also not known to what extent oral and gut microbial disease markers might converge in terms of their

¹Department of Rheumatology and Clinical Immunology, Peking Union Medical College Hospital, Chinese Academy of Medical Sciences and Peking Union Medical College, Beijing, China. ²BGI-Shenzhen, Shenzhen, China. ³Shenzhen Key Laboratory of Human Commensal Microorganisms and Health Research, BGI-Shenzhen, Shenzhen, China. ⁴Shenzhen Engineering Laboratory of Detection and Intervention of Human Intestinal Microbiome, BGI-Shenzhen, Shenzhen, China. ⁵Department of Biology, University of Copenhagen, Copenhagen, Denmark. ⁶School of Bioscience and Biotechnology, South China University of Technology, Guangzhou, China. ⁷BGI Education Center, University of Chinese Academy of Sciences, Shenzhen, China. ⁸Qingdao University–BGI Joint Innovation College, Qingdao University, Qingdao, China. ⁹Department of Mathematical Sciences, Binghamton University, State University of New York, Binghamton, New York, USA. ¹⁰Princess Al-Jawhara Al Brahim Centre of Excellence in Research of Hereditary Disorders (PACER-HD), Faculty of Medicine, King Abdulaziz University, Jeddah, Saudi Arabia. ¹¹Macau University of Science and Technology, Taipa, Macau, China. ¹²Department of Rheumatology, Guangdong Hospital of Traditional Chinese Medicine, Guangzhou, China. ¹³These authors contributed equally to this work. Correspondence should be addressed to J.W. (wangj@genomics.org.cn), Y.L. (liyr@bgitechsolutions.com) or X.Z. (zxpumch2003@sina.com).

Received 29 January; accepted 29 June; published online 27 July 2015; doi:10.1038/nm.3914

composition or function, as this is not apparent from 16S rRNA gene analyses of fecal or dental samples from individuals with RA^{16–19}.

RESULTS

Gut microbial dysbiosis is detectable in RA and is associated with clinical indices

To investigate the gut microbiome in RA patients, we carried out metagenomic shotgun sequencing of 212 fecal samples (77 treatment-naive individuals with RA and 80 unrelated healthy controls; 17 treatment-naive individuals with RA paired with 17 healthy relatives; and 21 samples from DMARD-treated individuals with RA) (Supplementary Tables 1 and 2). We then integrated the data into an existing gut microbial reference-gene catalog to obtain a set of 5.9 million genes, which allowed for saturation mapping of the sequencing reads ($80.3\% \pm 2.3\%$, mean \pm s.d.)¹². Gut microbial diversity and richness were similar between the 77 treatment-naive individuals with RA and 80 unrelated healthy controls (Supplementary Fig. 1). The duration of RA did not significantly separate the individuals with RA in principal-coordinate analysis at the genus level or in permutational analysis of variance (PERMANOVA) of the gene profile (Supplementary Fig. 2 and Supplementary Table 3).

To delineate features of the RA-associated gut microbiome, we identified 117,219 gene markers that were differentially enriched in RA patients versus controls (Wilcoxon rank-sum test, false discovery rate (FDR) < 0.3) and clustered the genes into metagenomic linkage groups (MLGs) on the basis of their correlated abundance variation among samples²⁰. The 88 MLGs that contained at least 100 genes (Supplementary Fig. 3 and Supplementary Table 4) separated RA-enriched and control-enriched MLGs along the vector for RA status in canonical correspondence analysis (CCA) (Supplementary Fig. 4), confirming that they were associated mainly with RA status, rather than with other complicating factors.

A cluster containing *Veillonella* and *Haemophilus* strains (Spearman's correlation coefficient > 0.3), along with other MLGs including *Klebsiella pneumoniae*, *Bifidobacterium bifidum*, *Sutterella wadsworthensis* and *Megamonas hypermegale*, were enriched in the healthy controls compared with the RA subjects (Supplementary Fig. 3). In contrast, the RA-enriched MLGs formed a large cluster including *Clostridium asparagiforme*, *Gordonibacter pamelaeeae*, *Eggerthella lenta* and *Lachnospiraceae bacterium*, as well as small clusters or single MLGs containing strains such as *Bifidobacterium dentium*, *Lactobacillus* sp. and *Ruminococcus lactaris*. A few control MLGs negatively correlated with RA MLGs (e.g., *K. pneumoniae* and *Bacteroides* sp., *B. bifidum* and *R. lactaris*) (Supplementary Fig. 3), suggesting an antagonistic or mutually exclusive relationship.

The RA gut was enriched in Gram-positive bacteria and depleted of Gram-negative bacteria, including some Proteobacteria and Gram-negative Firmicutes of the Veillonellaceae family (Supplementary Fig. 3). A few phylogenetically related strains showed different directions of enrichment. For instance, Con-1511 (most closely related to *Bacteroides plebeius*) was enriched in controls, whereas a *Bacteroides* sp. (most closely related to *Bacteroides* sp. 20_3) was enriched in patients (Supplementary Fig. 3 and Supplementary Table 4). These results partly confirm and extend the results of previous studies based on 16S rRNA sequencing^{16,17,19} (Supplementary Table 5).

Consistent with results from principal-coordinate analysis and PERMANOVA at the genus and gene levels (Supplementary Fig. 2a and Supplementary Table 3), the abundance of only one gut MLG was different among treatment-naive individuals with RA of different durations (Kruskal-Wallis test, $P < 0.05$; Supplementary Fig. 2b).

In contrast, the abundance of three dental MLGs and ten salivary MLGs changed with disease duration, with RA-enriched MLGs often increasing and control-enriched MLGs decreasing as a function of the duration of RA (Supplementary Fig. 2c,d). None of the MLGs containing 100 or more genes was annotated to *Prevotella copri* (Supplementary Fig. 3 and Supplementary Table 4), in agreement with its existence and genomic variability in the healthy population^{10,13,19,21–25}. Yet according to the *P. copri* NCBI reference draft genome (DSM 18205), there was a trend toward increased abundance of *P. copri* as a function of RA duration in the first year (Supplementary Fig. 5), consistent with its reported expansion in subjects with new-onset RA (6 weeks to 6 months)¹⁹.

In line with the relative depletion of Gram-negative bacteria in RA, Kyoto Encyclopedia of Genes and Genomes (KEGG) modules involved in lipopolysaccharide biosynthesis, lipopolysaccharide transport, and secretion systems (type II, type IV and type VI) were more abundant in samples from healthy controls (Fig. 1 and Supplementary Table 6). In contrast, enrichment of the reductive acetyl-CoA pathway in individuals with RA was consistent with the overabundance of acetate-producing bacteria such as *Clostridium* spp. and modules for converting acetate to methane (Fig. 1 and Supplementary Table 6). Together, these results indicate that the gut microbiome of individuals with RA is distinct from that of healthy individuals.

To explore the diagnostic or prognostic value of the gut microbiome for RA, we investigated numerical covariations between the relative abundance of the MLGs and clinical indices using Spearman's correlation (Supplementary Fig. 4). The abundance of RA-enriched MLGs such as *C. asparagiforme* and *Bacteroides* sp. was positively correlated with titers of immunoglobulin A (IgA), and that of an unclassified *Lactobacillus* sp. (most likely *L. salivarius*; Supplementary Table 4) positively correlated with titers of the major serum immunoglobulin, IgG (Supplementary Fig. 4). A positive correlation between RA-2166 (which is related to *Enterococcus faecalis*; Supplementary Table 4) and platelet count (Supplementary Fig. 6) was detected, which is consistent with prior reports showing that *E. faecalis* binds platelets^{26,27}.

Additional correlations with clinical indices were found with MLGs enriched in controls but also present in a fraction of individuals with RA (Supplementary Table 4). The abundance of Con-7851 and *B. bifidum* correlated negatively with titers of IgA and IgG; Con-1511, Con-2297, Con-2316 and an unclassified *Haemophilus* sp. (most closely related to *B. plebeius*, *Streptococcus australis*, *Veillonella* sp. oral taxon 158 and *Haemophilus parainfluenzae*, respectively; Supplementary Table 4) negatively correlated with titers of the RA-specific autoantibodies anticyclic citrullinated peptide (anti-CCP) and rheumatoid factor (RF) (Supplementary Fig. 6). Furthermore, cross-validated random forest models based on the gut MLGs were able to fit the clinical indices with a small R^2 value (Supplementary Table 7), which indicated that the gut MLGs could to some extent reflect the clinical variations among these subjects.

Oral microbial dysbiosis is present in RA and is associated with clinical indices

Next we investigated whether dysbiosis is also evident in the oral microbiome. We shotgun-sequenced 105 dental and 98 saliva samples (dental: 54 treatment-naive RA, 51 controls; saliva: 51 RA, 47 controls; 69 of the subjects had a complete set of fecal, dental and salivary samples) (Supplementary Tables 1 and 2). *De novo* assembly of these sequences led to a gene catalog of 3.2 million genes, with $76.6\% \pm 1.8\%$ and $70.7\% \pm 7.3\%$ (mean \pm s.d.) mapping of the dental and salivary sequencing reads, respectively.

RA status had the strongest effect on the dental and salivary microbiomes among all available phenotypes (lowest *P* value in PERMANOVA; **Supplementary Tables 8 and 9**). We identified 371,990 and 258,055 gene markers enriched in either healthy controls

or individuals with RA from the dental and salivary samples, respectively (Wilcoxon rank-sum test, FDR < 0.1). MLGs were constructed in the same way as for the fecal samples²⁰, making this, to our knowledge, the first MGWAS on the oral microbiome.

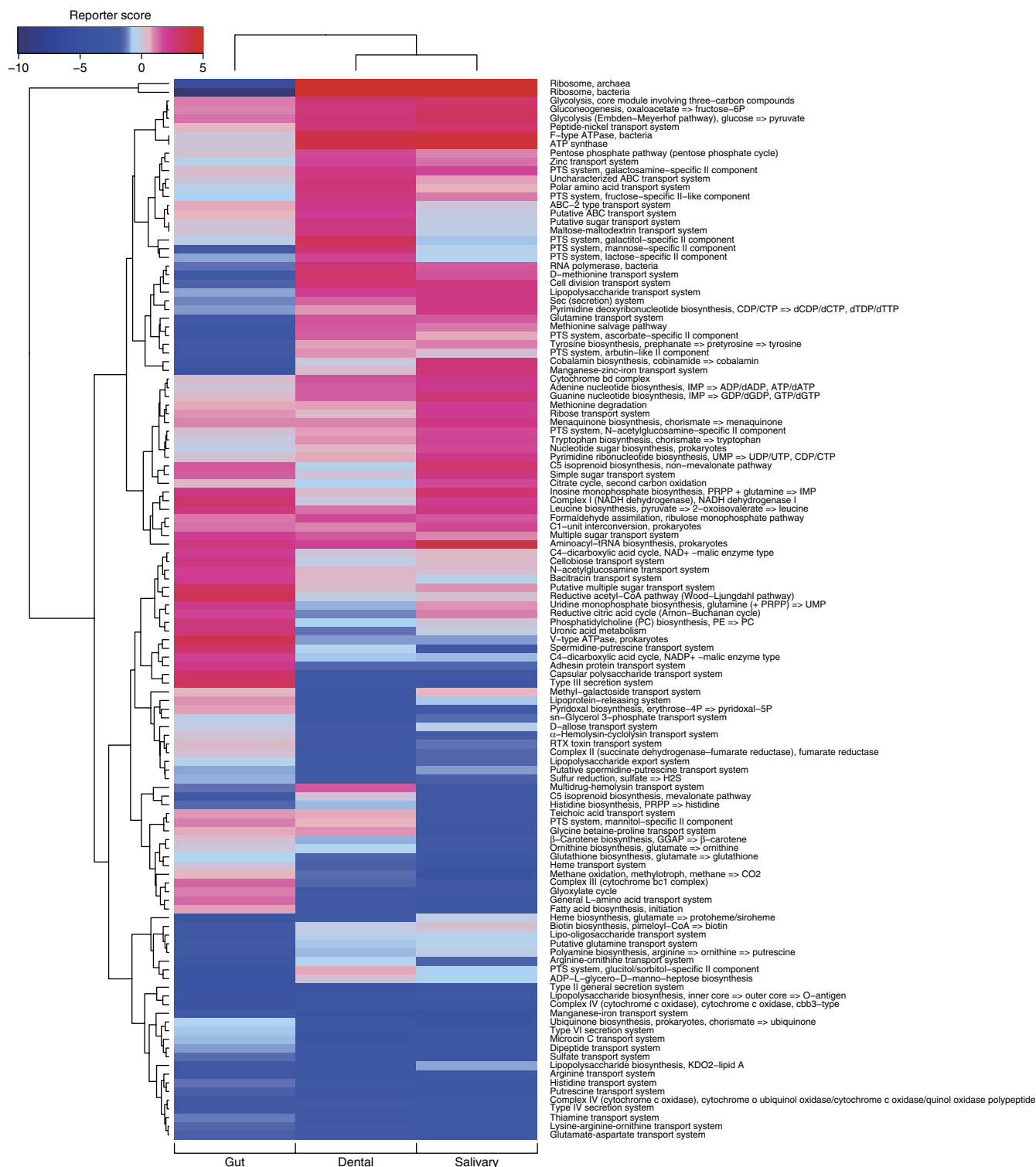


Figure 1 Microbial dysbiosis in the gut, dental plaques and saliva of individuals with RA. Heat map of KEGG modules differentially enriched between samples of feces ($n = 157$), dental plaques ($n = 105$) and saliva ($n = 98$) from RA and control subjects (reporter score ≥ 1.7 ; **Supplementary Tables 5, 15 and 16**). The KEGG orthology group modules and body sites are ordered by unsupervised hierarchical clustering. Blue, enriched in controls; red, enriched in RA subjects. Modules missing from one or more body sites are not plotted.

The 171 dental and 142 salivary MLGs that contained at least 100 genes (Fig. 2 and Supplementary Tables 10 and 11) were separated into control-enriched and RA-enriched MLGs along the vector for RA status in CCA (Supplementary Fig. 4b,c), confirming their association with RA. The dental MLGs were highly interconnected in the controls, whereas the salivary MLGs were more interconnected in the RA patients than in the controls (Fig. 2, Spearman's correlation > 0.55). *Veillonella* MLGs were overrepresented in the gut of healthy controls (Supplementary Fig. 3) but were elevated in the dental plaques and saliva of individuals with RA (Fig. 2 and Supplementary Tables 10 and 11). These *Veillonella* MLGs possibly belonged to different species (Supplementary Table 12). MLGs annotated to *Haemophilus* spp. remained enriched in the control samples at all three sites, although the exact strain could differ between the gut and oral sites (Supplementary Tables 4 and 10–12). MLGs corresponding to common childhood endocarditis-related

Gram-negative bacteria (*Haemophilus*, *Aggregatibacter*, *Cardiobacterium*, *Eikenella*, *Kingella* (HACEK)) were enriched in the control dental and/or salivary samples (Fig. 2 and Supplementary Tables 10 and 11). The peptidyl-arginine deiminase (PAD)-encoding *Porphyromonas gingivalis* was enriched in control saliva and, to a lesser extent, in control dental plaques (Fig. 2 and Supplementary Tables 10 and 11), in agreement with recent studies that did not find an association between *P. gingivalis* or its PAD and RA^{18,28}. *Rothia* spp. have been implicated in treatable periodontitis, endocarditis, and joint infections^{29–31}. We found that *Rothia aerea* was enriched in control saliva, *Rothia mucilaginoso*-like MLGs were enriched in RA saliva and dental plaques (RA-8122 and RA-15331, respectively), and RA-24511 (*Rothia dentocariosa*) was enriched in RA dental plaques (Fig. 2 and Supplementary Tables 10 and 11). Anaerobes such as *Lactobacillus salivarius*, *Atopobium* spp. and *Cryptobacterium curtum* were enriched in both salivary and

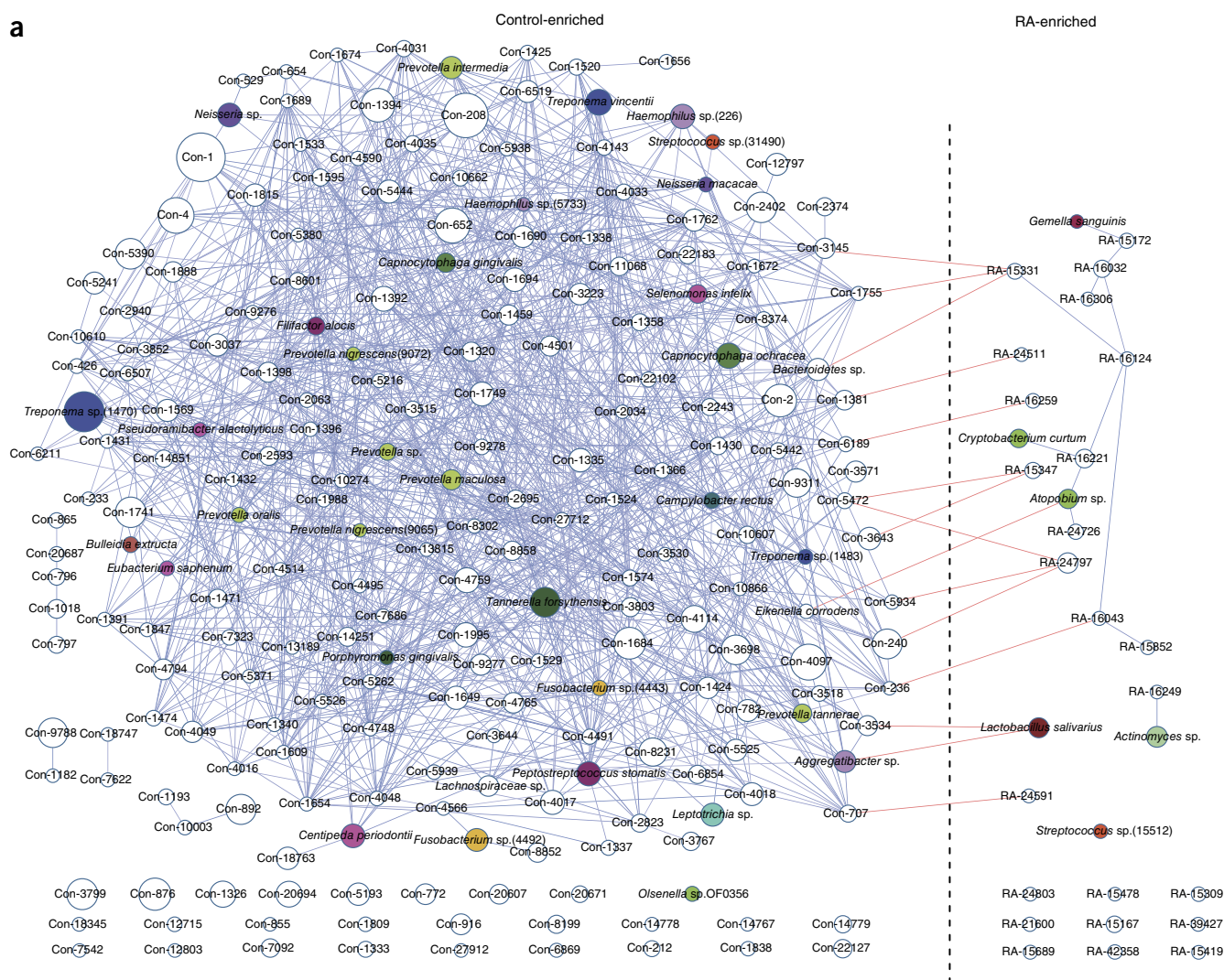


Figure 2 Oral MLGs enriched in dental and salivary samples of RA subjects and controls. (a,b) MLGs (≥ 100 genes) enriched in oral (a) and salivary (b) samples (for dental samples, $n = 51$ controls and 54 RA; for salivary samples, $n = 47$ controls and 51 RA), colored according to family. MLG identification numbers are listed in parentheses if more than one MLG annotated to the same species or unclassified species in a genus (sp.). Possible strain names are listed in Supplementary Tables 10 and 11 for all MLGs with more than 50% of genes annotated to the strain(s), even if the criteria for pinpointing a species or a genus were not met (Online Methods). Sizes of nodes reflect the number of genes in the MLGs (100–4,667 for dental, 102–4,996 for salivary). Blue edges, Spearman's correlation coefficient > 0.55 , $P < 0.05$; red edges, Spearman's correlation coefficient < -0.35 for dental and < -0.5 for salivary, $P < 0.05$.

dental samples from subjects with RA, in contrast to aerobes such as *Nesseria* spp. and *R. aeria*, which were enriched in controls (Fig. 2 and Supplementary Tables 10 and 11). Strains enriched in control saliva such as *Lactococcus* sp., Con-1, Con-80 and *Cardiobacterium hominis* negatively correlated with MLGs enriched in RA samples, including *Atopobium* sp. and *Veillonella* strains (Spearman's correlation coefficient <-0.5 ; Fig. 2b). Control oral MLGs such as *Capnocytophaga ochraea* and *Leptotrichia* sp. and RA-enriched *Selenomonas flueggei* had taxa similar to those reported in previous 16S studies^{18,32,33} (Supplementary Table 5). Collectively, these findings indicate that microbial markers enriched in control and RA samples were differentially distributed among the fecal, dental and salivary microbiomes, although the dental and salivary sites showed greater similarity to each other.

Next we computed covariations between the relative abundance of dental and salivary MLGs and clinical indices for RA, and we noted the separation between control-enriched and RA-enriched MLGs on the

basis of the clinical indices (Supplementary Figs. 7 and 8). A number of MLGs enriched in the healthy control dental samples, including *Aggregatibacter* sp., *Haemophilus* spp., *Neisseria* spp. and *Prevotella intermedia*, negatively correlated with C-reactive protein (CRP), a marker for acute inflammation (Supplementary Fig. 7). Healthy control MLGs such as Con-3223 and Con-5472 negatively correlated with both CRP and anti-CCP autoantibodies, whereas RA-enriched *Actinomyces* sp. and RA-16259 positively correlated with anti-CCP autoantibodies. Con-6189 and Con-8374 negatively correlated with CRP and RF, an autoantibody directed against the Fc region. In the saliva, RA-11340 positively correlated with anti-CCP, whereas Con-658, Con-662 and *Haemophilus* spp. negatively correlated with anti-CCP (Supplementary Fig. 8). Con-2134 negatively correlated with RF, whereas RA-5059, RA-7901 and *Prevotella* spp. positively correlated with RF.

Cross-validated random forest models based on dental or salivary MLGs were able to fit clinically measured indices such as DAS28, CRP, anti-CCP and IgG in the cohort (Supplementary Tables 13 and 14),

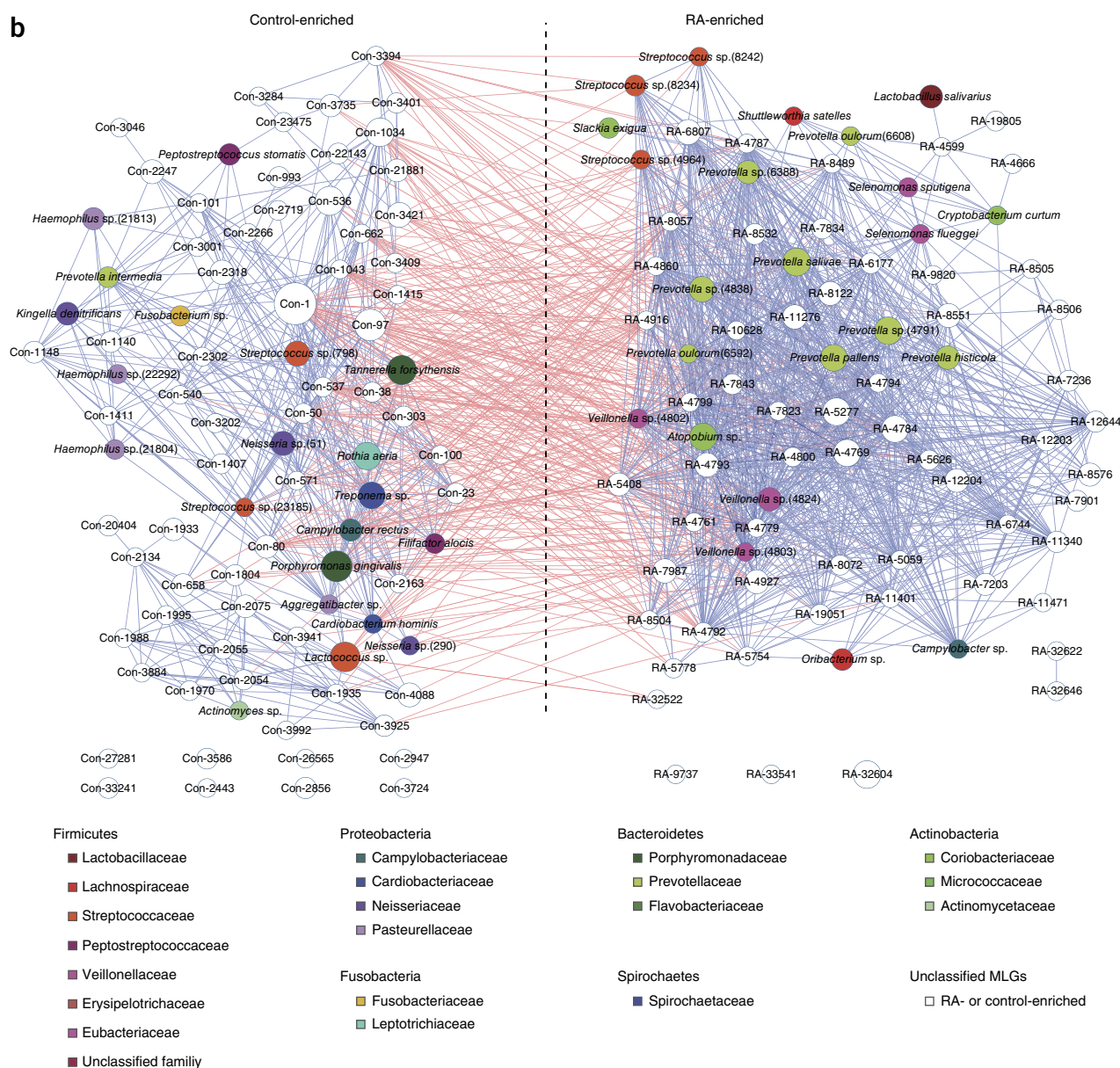


Figure 2 (Continued)

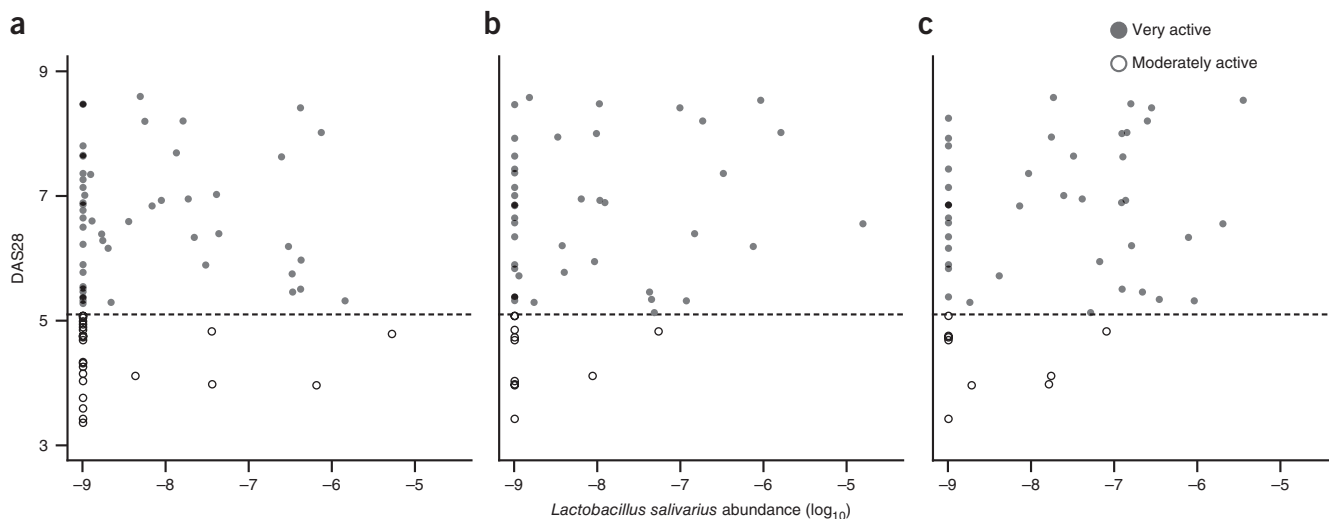


Figure 3 Patient stratification on the basis of RA-associated bacteria. (a–c) Relative abundance of *L. salivarius* MLGs in fecal (a), dental (b) and salivary (c) samples from patients with very active (filled circles) and moderately active (open circles) RA ($P = 0.017$, 0.036 and 0.084 , respectively; Wilcoxon rank-sum test). The MLG identification numbers are 2169 (gut), 16600 (dental) and 4643 (salivary) (Supplementary Tables 4, 10 and 11). The disease classification followed EULAR criteria: moderate, $3.2 < \text{DAS28} \leq 5.1$; very active, $\text{DAS28} > 5.1$ (Supplementary Table 1).

which indicated that measured oral MLGs could be used to derive these clinical indices in this cohort. Thus, although the oral microbiome may be influenced by additional factors such as diet and oral hygiene, our results indicate that, consistent with clinical observations, the oral microbiome deviates from a healthy status in individuals with RA.

Concordance between gut and oral microbiomes

To examine the concordance and divergence of the microbiome at different body sites in individuals with RA, we analyzed functional modules using the KEGG database. Like the gut microbiome, the dental and salivary microbiomes of RA patients were relatively depleted of type II, type IV and type VI secretion systems; arginine and putrescine transport systems; and synthesis of putrescine and spermidine from arginine (Fig. 1; Supplementary Tables 5, 15 and 16; and Supplementary Note).

The module related to ubiquinone (coenzyme Q) synthesis was more abundant in the control oral and gut samples, whereas menaquinone (vitamin K_2) synthesis was elevated in individuals with RA at the same sites (Fig. 1 and Supplementary Tables 5, 15 and 16), suggesting more anaerobic respiration. Complex I (NADH dehydrogenase) of the respiratory chain was enriched in RA subjects, whereas Complexes III and IV were relatively depleted in these subjects (Fig. 1). RA saliva samples were enriched for iron(III) transport instead of iron(II) transport systems (Supplementary Fig. 9a). Salivary MLGs that correlated with iron(III) transport included RA-5626 and RA-5778 (which are most closely related to *Solobacterium moorei*; Supplementary Table 11), whereas iron(II) transport (manganese-iron transport system) was associated with control-enriched MLGs such as gut *K. pneumoniae*, dental and salivary *Haemophilus* spp., *Aggregatibacter* spp. and *Eikenella corrodens* (Supplementary Tables 17 and 18). Zinc transport systems were enriched in the control fecal samples but were also enriched in the RA oral samples compared with control oral samples (Fig. 1; Supplementary Fig. 9a; and Supplementary Tables 5, 15 and 16).

The healthy oral microbiome was enriched in modules involved in sulfur reduction and sulfate transport (Fig. 1; Supplementary Fig. 9b; Supplementary Tables 15 and 16; and Supplementary Note).

KEGG orthology groups responsible for hydrogen sulfide production correlated with control MLGs such as *Aggregatibacter* spp., *Haemophilus* spp. and *Kingella dinitrificans*; in contrast, *Bacteroides* spp. were enriched in the gut of RA subjects (Supplementary Tables 17 and 18). Alterations in nitrogen, iron and sulfur metabolism in RA also manifested as differential enrichment of heme transport and synthesis pathways in gut and oral sites between control and RA subjects (Fig. 1 and Supplementary Fig. 9c).

Molecular mimicry of RA-associated antigens such as Collagen XI and HLA-DRB1*0401 (ref. 34) by gut microbial genes from *Clostridium*, *Eggerthella*, *Bacteroides* and *Citrobacter* was also suggested, with a number of the genes belonging to MLGs enriched in RA gut samples (Supplementary Fig. 10 and Supplementary Table 19). In contrast, only one gut microbial gene contained a motif similar to the spondyloarthritis-related antigen HLA-B27. Although the signal was more diverse in the oral microbiome, RA-enriched genes from *Atopobium*, *Oribacterium*, *Actinomyces* and *Cryptobacterium* mimicked motifs in Collagen XI and HLA-DRB1*0401, whereas few motifs similar to HLA-B27 could be found (Supplementary Fig. 10 and Supplementary Tables 20 and 21). Thus, both the gut and the oral microbiome might contribute to RA through molecular mimicry of self-antigens^{34,35}.

Despite differences between the gut and oral bacterial taxa associated with RA, *Haemophilus* spp. were overrepresented in the control samples from all gut and oral sites and negatively correlated with amounts of serum anti-CCP, RF and CRP (Supplementary Figs. 6–8). *L. salivarius* was consistently enriched in individuals with RA. Amounts of gut and salivary *L. salivarius* positively correlated with IgG levels, and the dental *L. salivarius* showed the second highest odds ratio among all dental MLGs (Supplementary Table 10). Furthermore, *L. salivarius* was more abundant in very active cases of RA ($\text{DAS28} > 5.1$) compared with mild to moderately active ($\text{DAS28} \leq 5.1$) cases (Fig. 3), underscoring its potential for use in patient stratification.

To better understand the distribution of RA-associated bacteria across body sites, we computed the correlation of the relative abundances of fecal, dental and salivary MLGs among samples ($n = 69$).

L. salivarius (*Lactobacillus* sp. in the gut; **Supplementary Table 4**) showed a positive correlation among all three sites (**Fig. 4, Supplementary Fig. 11** and **Supplementary Table 12**), confirming its presence in multiple body sites. The RA-enriched gut bacteria *B. dentium* and RA-6364 negatively correlated with a number of control-enriched dental MLGs (Spearman's correlation < -0.4 ; **Fig. 4a**). The MLG Con-5303, which was enriched in control gut samples, positively correlated with many control-enriched dental MLGs such as *Haemophilus* spp., *Aggregatibacter* sp. and *P. intermedia* (Spearman's correlation > 0.4). The RA-enriched gut bacteria *C. asparagiforme* negatively correlated with control salivary MLGs *P. intermedia*, *Haemophilus* spp. and *Kingella denitrificans* and positively correlated with RA salivary MLGs such as RA-8057 and RA-8551 (**Fig. 4b**). A similar pattern was observed for RA-enriched gut MLGs *Bacteroides* sp., *B. dentium* and *Lactobacillus* sp. The control salivary MLG *Lactococcus* sp. correlated negatively with an RA gut *Bacteroides* sp. and positively with control gut MLGs including Con-5303 and *K. pneumoniae*. Together, these results demonstrate covariation of bacteria at different body sites in individuals with RA and indicate that the microbiome at a given site contains information for other sites.

Microbiome-based identification of RA patients

To illustrate the diagnostic value of the RA-associated microbiome, we first constructed random forest disease classifiers based on the gut MLGs (**Fig. 5**). Tenfold cross-validation was done five times on the cohort ($N = 157$), and the final model contained 8 of the 88 gut MLGs (**Supplementary Fig. 12** and **Supplementary Table 4**), leading to an area under the receiver operating curve (AUC) of 0.940 (specificity, 0.922; sensitivity, 0.838; **Fig. 5a**). The model also classified an additional set of samples comprising consanguineous and nonconsanguineous case-control pairs ($N = 34$) (**Fig. 5b**). Thus, the performance of our model with

gut MLGs was comparable to that of existing classifiers based on RA serum markers³⁶.

Similarly, six dental MLGs and two salivary MLGs performed well in our cohort (Dental: AUC, 0.870; specificity, 0.860; sensitivity, 0.800. Salivary: AUC, 0.814; specificity, 1.000; sensitivity, 0.702; **Fig. 5d,f, Supplementary Fig. 12** and **Supplementary Tables 10** and **11**). Of the two salivary MLGs, RA-32522 was present only in individuals with RA and their healthy relatives, whereas the unclassified *Lactococcus* sp. was present in the unrelated healthy controls. Salivary *Lactococcus*

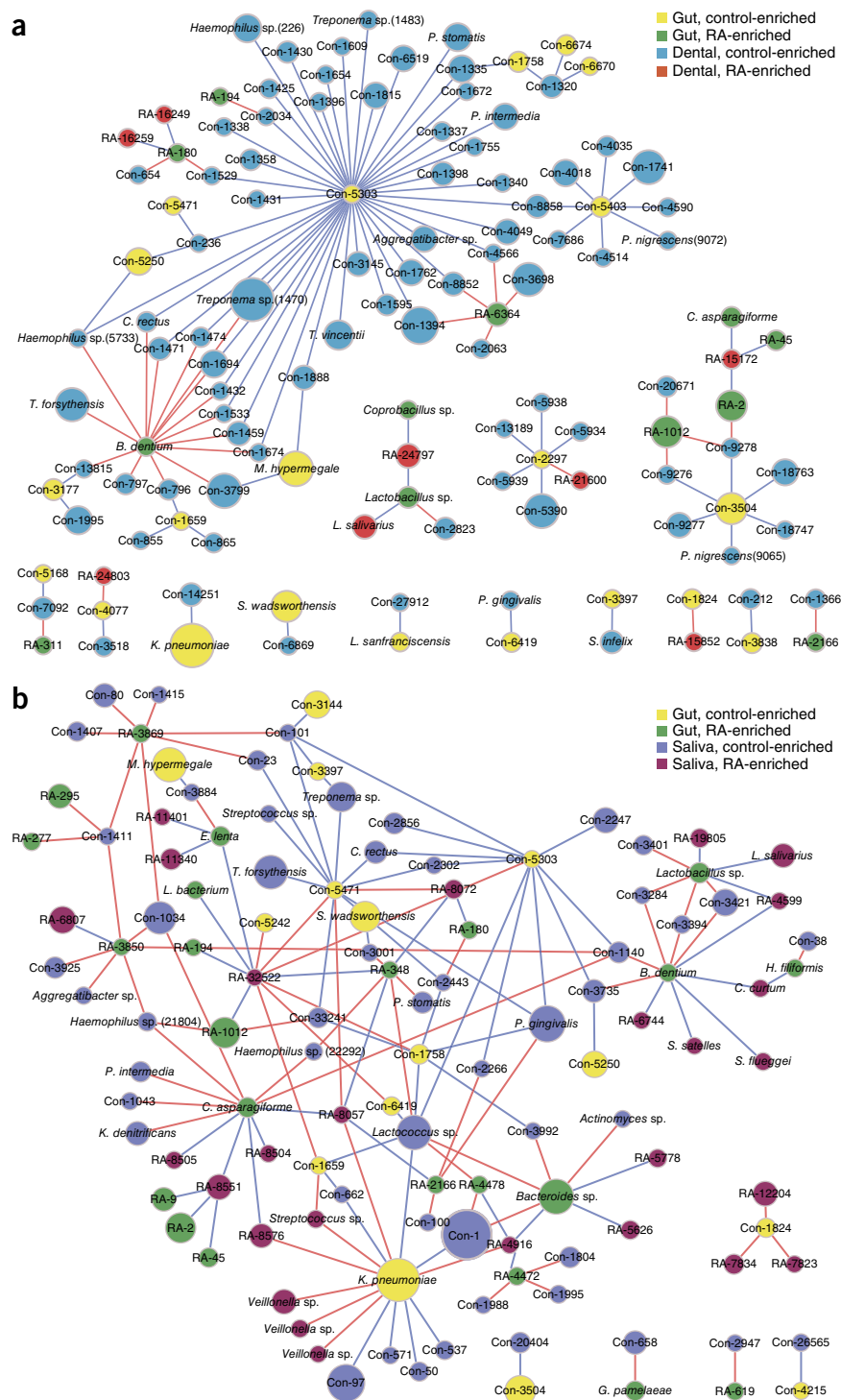


Figure 4 Correlation between gut and oral MLGs. **(a,b)** Spearman's correlation between the relative abundances of gut and dental **(a)** or gut and salivary **(b)** MLGs (≥ 100 genes) were calculated for subjects with full sets of fecal, dental and salivary samples ($n = 69$). Sizes of nodes reflect the number of genes in each MLG. MLGs are colored according to body site and enrichment (yellow, control gut; green, RA gut; blue, control dental; red, RA dental; purple, control saliva; magenta, RA saliva). MLG identification numbers are listed in parentheses if more than one MLG annotated to the same species or unclassified species in a genus (sp.). Blue edges, Spearman's correlation coefficient > 0.4 , $P < 0.05$; red edges, Spearman's correlation coefficient < -0.4 , $P < 0.05$.

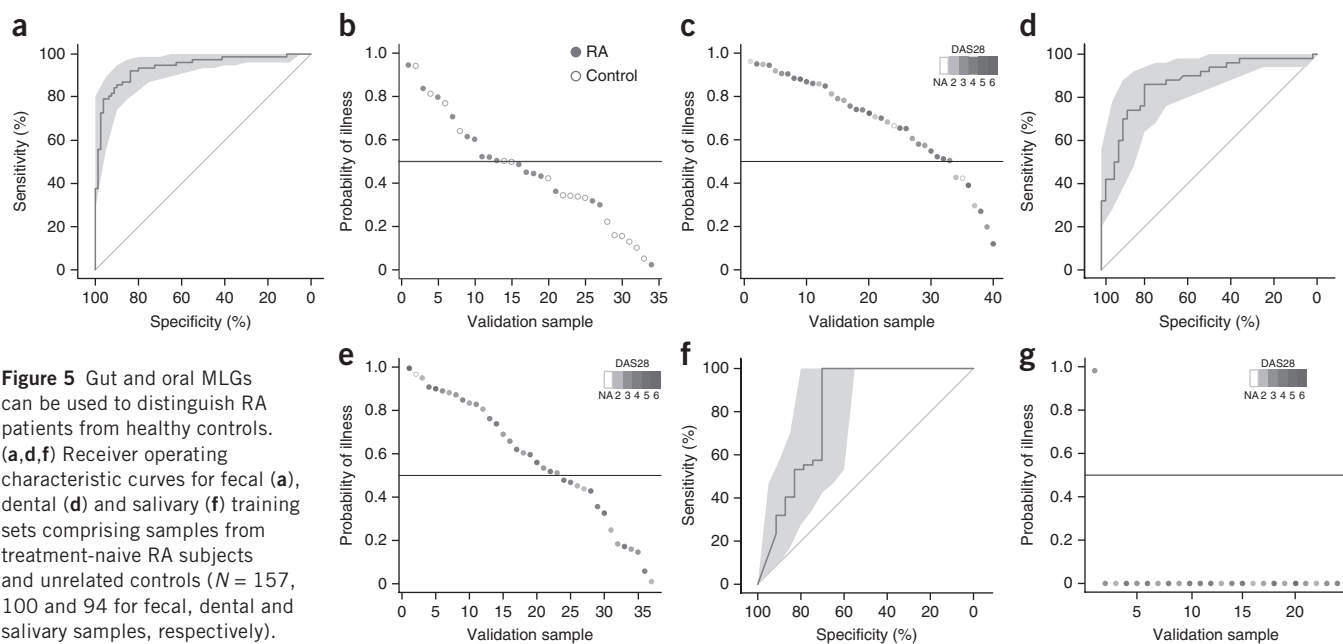


Figure 5 Gut and oral MLGs can be used to distinguish RA patients from healthy controls. **(a,d,f)** Receiver operating characteristic curves for fecal **(a)**, dental **(d)** and salivary **(f)** training sets comprising samples from treatment-naïve RA subjects and unrelated controls ($N = 157$, 100 and 94 for fecal, dental and salivary samples, respectively). $AUC = 0.9396$ for fecal, 0.8702 for dental and 0.8135 for salivary samples. The 95% confidence intervals (CIs) are shown as shaded areas. **(b)** Classification of fecal samples from 17 controls and 17 RA subjects, either consanguineous or nonconsanguineous relatives. Open circles, controls; filled circles, RA subjects. **(c,e,g)** Classification of fecal **(c)**, dental **(e)** and salivary **(g)** samples from DMARD-treated RA patients ($N = 40$, 37 and 24 for fecal, dental and salivary samples, respectively), shaded on a scale relative to DAS28. NA (no shading), DAS28 not available. The classification results for all samples are listed in **Supplementary Table 1**. Diagonal lines in graphs mark an AUC of 0.5 (i.e., random classification). Horizontal lines mark the probability cutoff (0.5).

and RA-32522 also correlated with a number of MLGs in the gut (**Fig. 4b** and **Supplementary Table 11**). When classification based on two sites was used to override the few misclassifications based on the third site, no subjects were misclassified except for one related control (**Supplementary Table 1**); this highlights the power of examining the microbiome at multiple sites. Moreover, testing the MLG classifiers on samples from DMARD-treated RA patients still correctly identified the individuals as having RA for most of the fecal and dental samples (**Fig. 5c,e,g** and **Supplementary Table 1**). However, dental samples with low disease activity (DAS28) were often classified as healthy, consistent with clinical relief of periodontitis after treatment of RA.

DMARD treatment partially restores a healthy RA microbiome

To examine whether DMARD treatment restores a healthy microbiome, we compared the relative abundance of control and RA gut and oral MLGs before and after treatment (for 3 months in 34 individuals and for other time periods for six fecal samples) (**Supplementary Tables 1** and **2**). Consistent with results from the RA classifiers, more dental and salivary MLGs showed significant changes in abundance than did gut MLGs ($P < 0.05$, Wilcoxon rank-sum test; **Fig. 6**

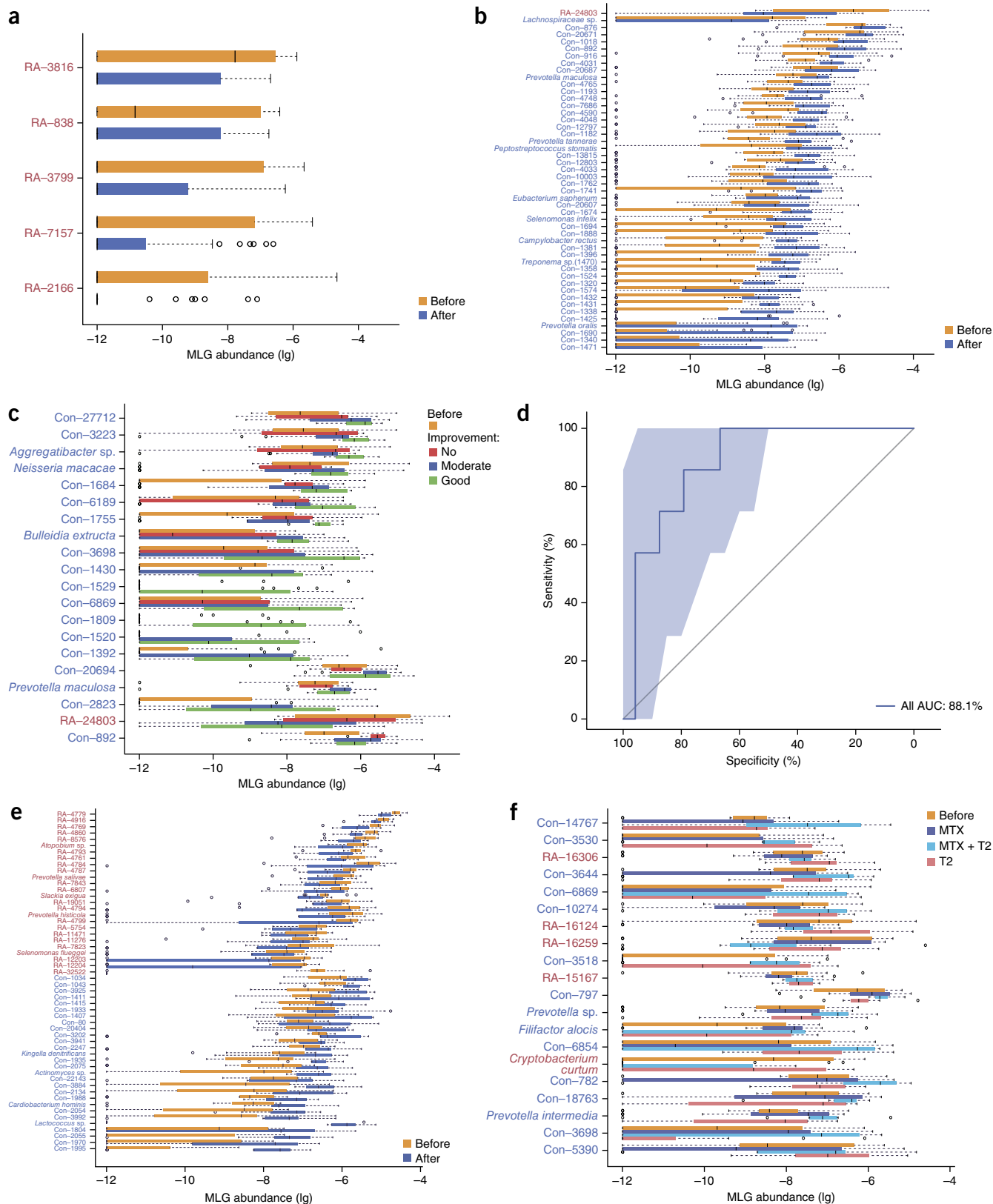
and **Supplementary Fig. 13**). In the dental plaques, amounts of RA-24803 were decreased after DMARD therapy, especially in patients who showed good or moderate improvement after treatment compared to those with no improvement ($P < 0.05$, Wilcoxon rank-sum test; **Fig. 6b,c**), according to the European League Against Rheumatism (EULAR) response criteria based on DAS28 reduction. MLGs enriched in healthy control dental samples, including *Prevotella maculosa*, increased in RA patients after treatment, especially in those who showed good or moderate improvement. Among the control MLGs that were differentially enriched in dental samples of patients with good, moderate or no improvement after DMARD therapy were MLGs (unclassified *Aggregatibacter* sp., Con-3223 and Con-6189) that negatively correlated with CRP, anti-CCP or RF, implying clinically relevant improvement in the dental microbiome.

Cross-validated random forest models based on gut, dental or salivary MLGs in before-treatment samples were able to distinguish patients who showed good or moderate improvement from patients who showed no improvement after DMARD therapy (dental: AUC , 0.881; specificity, 1.000; sensitivity, 0.667; **Fig. 6d**, **Supplementary Fig. 14** and **Supplementary Table 22**). Gut MLGs used in the improvement

Figure 6 The microbiome is altered after DMARD treatment. **(a)** Control gut MLGs (≥ 100 genes; **Supplementary Fig. 3**) affected by DMARD treatment ($P < 0.05$, paired Wilcoxon rank-sum test, $N = 32$). **(b)** Control dental MLGs (≥ 100 genes; **Fig. 2a**) affected by DMARD treatment ($P < 0.05$, paired Wilcoxon rank-sum test, $N = 15$). **(c)** Control dental MLGs differentially enriched in patients with good, moderate or no improvement ($N = 9$, 21 or 10, respectively; $P < 0.05$ between good and moderate, good and unimproved, and moderate and unimproved, Wilcoxon rank-sum test). **(d)** Receiver operating characteristic curve for prediction of improvement after DMARD treatment from before-treatment dental samples. Tenfold cross-validation with a random forest classifier was done five times, and 17 MLGs were selected (**Supplementary Table 10**). $N = 24$ for good or moderate improvement, $N = 7$ for no improvement (**Supplementary Table 22**). $AUC = 0.881$; 95% CI shown as a shaded area. The diagonal line marks an AUC of 0.5 (i.e., random classification). **(e)** Control salivary MLGs (≥ 100 genes; **Fig. 2b**) affected by DMARD treatment ($P < 0.05$, paired Wilcoxon rank-sum test, $n = 10$). MLGs enriched in control samples are shown in blue text, and MLGs enriched in RA samples are in red text (**a–c,e,f**). **(f)** Control dental MLGs differentially enriched in patients after treatment with MTX, MTX + T2 or T2 ($N = 14$, 10 or 12, respectively; $P < 0.05$ between MTX and MTX + T2, between MTX and T2, and between MTX + T2 and T2, Wilcoxon rank-sum test). In all box plots, interquartile ranges (IQRs; boxes), medians (dark vertical lines in boxes), the lowest and highest values within a range 1.5 times the IQR from the first and third quartiles (whiskers) and outliers beyond the whiskers (circles) are shown.

classifiers included Con-5303, Con-3144 and *Holdemania filiformis*, which correlated with dental and salivary MLGs (Fig. 4 and Supplementary Table 4). Oral MLGs included in the classifiers, including *Veillonella* spp., also correlated with gut MLGs (Fig. 4 and

Supplementary Tables 10 and 11). Fecal, dental and salivary samples from RA patients who showed improvement contained a greater number of virulence factors (according to the virulence factor database³⁷) than did those from patients with no improvement, and the dental and



salivary control samples had more virulence factors than the RA patient samples (**Supplementary Fig. 15** and **Supplementary Tables 23–25**). In summary, DMARD treatment partially modified the RA-associated microbiome, and the associated MLGs might facilitate the prediction and evaluation of treatment effects.

Most of the treated RA patients received methotrexate (MTX), glycosides of the traditional Chinese medicinal component *Tripterygium wilfordii* (thunder god vine) (T2)^{38–40} or both (MTX + T2) for DMARD treatment (**Supplementary Tables 1** and **22**). MLGs enriched in RA gut such as *H. filiformis* and *Bacteroides* sp. were reduced to a greater extent after treatment with T2 than after treatment with MTX or MTX + T2 (**Supplementary Fig. 13b**). MLGs enriched in control dental samples, including *P. intermedia*, were more abundant in patients treated with MTX + T2 than in those treated with T2 alone or MTX alone, whereas *Veillonella* sp. and RA-8489, enriched in RA saliva samples, were reduced to a greater extent in patients treated with T2 or with MTX + T2 (**Fig. 6f** and **Supplementary Fig. 13d**). These data suggest that distinct DMARDs modulate the gut and oral microbiome differently, although differences among RA patients remain likely.

DISCUSSION

Our MGWAS identified compositional and functional alterations in RA-associated gut and oral microbiomes that were partly relieved by DMARD treatment. Gut and oral MLGs correlated with each other and with clinical indices such as CRP, anti-CCP and RF, and they permitted preliminary classification of RA subjects. The dental and salivary microbiomes were altered, and these could be sampled easily at clinical visits or by the patients themselves. Our comprehensive survey of the gut and oral microbiomes in individuals with RA supports the notion that RA represents a state of chronic inflammation that might be provoked or aggravated by the overgrowth of pathogenic bacteria or a lack of immune-modulating commensal bacteria (**Supplementary Note**). These findings are a first step toward microbiome-based therapeutics and patient stratification in preclinical and clinical phases of RA. The identified markers need to be validated in larger and independent cohorts. Experiments in animal models and detailed *in vitro* characterizations of the strains will be necessary to elucidate whether a few of the identified markers are 'driver species' for the disease, although non-causal associations could still serve as markers for diagnosis or patient stratification. With further investigation of the possible mechanisms (**Supplementary Note**), microbiome-assisted diagnosis, prognosis and treatment could hold great promise for effective long-term management of autoimmune diseases such as RA, together with their accompanying dental and cardiovascular symptoms.

METHODS

Methods and any associated references are available in the [online version of the paper](#).

Accession codes. Metagenomic sequencing data for all samples have been deposited in the European Bioinformatic Institute (EBI) database under accession code [PRJEB6997](#).

Note: Any Supplementary Information and Source Data files are available in the online version of the paper.

ACKNOWLEDGMENTS

This research was supported by the Natural Science Foundation of China (grants 30890032 and 30725008 to Jun Wang and 81325019 to X.Z.), the Shenzhen Municipal Government of China (grant BGI20100001 to Jun Wang and grants JSGG20140702161403250 and DRC-SZ[2015]162 to Q.F.), the Danish Strategic Research Council (grant 2106-07-0021 to J.W.), an Ole Romer grant from the

Danish Natural Science Research Council and the Solexa project (272-07-0196 to J.W.), the Fund for Science and Technology Development (FDCT) from Macao (grant 077/2014/A2 to J.W.) and the Research Special Fund for Public Welfare Industry of Health (grant 2013202017 to X.Z.). The authors are very grateful to colleagues at BGI-Shenzhen for DNA extraction, library construction, sequencing and discussions.

AUTHOR CONTRIBUTIONS

X.Z., Yingrui Li and Jun Wang conceived and directed the project. X.Z., D.L., X. Wu, H.C., L.W., Q.-j.W., F.Z., W.Z. and Yongzhe Li made clinical diagnoses and performed treatment and sample collection. Z.L. and M.Z. managed the samples at BGI. D.Z., H.J., Q.F., D.W., Z.J., L.T., Yin Li, B.C., Z.L., Yanli Li, H.X., Junhua Li, Weineng Chen, S.T., Xiaoqiang Xu, X. Wang, X.C., S.L., Y.X., Jiyang Li and H.Z. performed bioinformatic analyses. X.Z., H.J. and L.L. wrote the manuscript. X.Q., G.L., W.X., L.X., Jun Li, Wanting Chen, Xun Xu, Y.Y., H.Y., Jian Wang, J.Y.A., K.K., T.L. and Q.H. contributed to data collection and text revision.

COMPETING FINANCIAL INTERESTS

The authors declare no competing financial interests.

Reprints and permissions information is available online at <http://www.nature.com/reprints/index.html>.

- McInnes, I.B. & Schett, G. The pathogenesis of rheumatoid arthritis. *N. Engl. J. Med.* **365**, 2205–2219 (2011).
- Raychaudhuri, S. *et al.* Five amino acids in three HLA proteins explain most of the association between MHC and seropositive rheumatoid arthritis. *Nat. Genet.* **44**, 291–296 (2012).
- Okada, Y. *et al.* Genetics of rheumatoid arthritis contributes to biology and drug discovery. *Nature* **506**, 376–381 (2014).
- McInnes, I.B. & Schett, G. Cytokines in the pathogenesis of rheumatoid arthritis. *Nat. Rev. Immunol.* **7**, 429–442 (2007).
- Viatte, S., Plant, D. & Raychaudhuri, S. Genetics and epigenetics of rheumatoid arthritis. *Nat. Rev. Rheumatol.* **9**, 141–153 (2013).
- Deane, K.D. & El-Gabalawy, H. Pathogenesis and prevention of rheumatic disease: focus on preclinical RA and SLE. *Nat. Rev. Rheumatol.* **10**, 212–228 (2014).
- Demoruelle, M.K., Deane, K.D. & Holers, V.M. When and where does inflammation begin in rheumatoid arthritis? *Curr. Opin. Rheumatol.* **26**, 64–71 (2014).
- Clemente, J.C., Ursell, L.K., Parfrey, L.W. & Knight, R. The impact of the gut microbiota on human health: an integrative view. *Cell* **148**, 1258–1270 (2012).
- Kamada, N., Seo, S.-U., Chen, G.Y. & Núñez, G. Role of the gut microbiota in immunity and inflammatory disease. *Nat. Rev. Immunol.* **13**, 321–335 (2013).
- Schloissnig, S. *et al.* Genomic variation landscape of the human gut microbiome. *Nature* **493**, 45–50 (2013).
- Faith, J.J. *et al.* The long-term stability of the human gut microbiota. *Science* **341**, 1237439 (2013).
- Li, J. *et al.* An integrated catalog of reference genes in the human gut microbiome. *Nat. Biotechnol.* **32**, 834–841 (2014).
- Yatsunenok, T. *et al.* Human gut microbiome viewed across age and geography. *Nature* **486**, 222–227 (2012).
- The Human Microbiome Project Consortium. A framework for human microbiome research. *Nature* **486**, 215–221 (2012).
- Wade, W.G. The oral microbiome in health and disease. *Pharmacol. Res.* **69**, 137–143 (2013).
- Liu, X., Zou, Q., Zeng, B., Fang, Y. & Wei, H. Analysis of fecal *Lactobacillus* community structure in patients with early rheumatoid arthritis. *Curr. Microbiol.* **67**, 170–176 (2013).
- Vahtovuori, J., Munukka, E., Korkeamäki, M., Luukkainen, R. & Toivanen, P. Fecal microbiota in early rheumatoid arthritis. *J. Rheumatol.* **35**, 1500–1505 (2008).
- Scher, J.U. *et al.* Periodontal disease and the oral microbiota in new-onset rheumatoid arthritis. *Arthritis Rheum.* **64**, 3083–3094 (2012).
- Scher, J.U. *et al.* Expansion of intestinal *Prevotella copri* correlates with enhanced susceptibility to arthritis. *Elife* **2**, e01202 (2013).
- Qin, J. *et al.* A metagenome-wide association study of gut microbiota in type 2 diabetes. *Nature* **490**, 55–60 (2012).
- Cotillard, A. *et al.* Dietary intervention impact on gut microbial gene richness. *Nature* **500**, 585–588 (2013).
- Nielsen, H.B. *et al.* Identification and assembly of genomes and genetic elements in complex metagenomic samples without using reference genomes. *Nat. Biotechnol.* **32**, 822–828 (2014).
- Hsiao, A. *et al.* Recovery from *Vibrio cholerae* infection. *Nature* **515**, 423–426 (2014).
- Bäckhed, F. *et al.* Dynamics and stabilization of the human gut microbiome in the first year of life. *Cell Host Microbe* **17**, 690–703 (2015).
- Franzosa, E.A. *et al.* Identifying personal microbiomes using metagenomic codes. *Proc. Natl. Acad. Sci. USA* **112**, E2930–E2938 (2015).
- Verschoor, A. *et al.* A platelet-mediated system for shuttling blood-borne bacteria to CD8 α^+ dendritic cells depends on glycoprotein GPIb and complement C3. *Nat. Immunol.* **12**, 1194–1201 (2011).

27. Yeaman, M.R. Platelets: at the nexus of antimicrobial defence. *Nat. Rev. Microbiol.* **12**, 426–437 (2014).
28. Konig, M.F., Paracha, A.S., Moni, M., Bingham, C.O. & Andrade, F. Defining the role of *Porphyromonas gingivalis* peptidylarginine deiminase (PPAD) in rheumatoid arthritis through the study of PPAD biology. *Ann. Rheum. Dis.* doi:10.1136/annrheumdis-2014-205385 (2014).
29. Michels, F. *et al.* Late prosthetic joint infection due to *Rothia mucilaginosa*. *Acta Orthop. Belg.* **73**, 263–267 (2007).
30. Verrall, A.J., Robinson, P.C., Tan, C.E., Mackie, W.G. & Blackmore, T.K. *Rothia aeria* as a cause of sepsis in a native joint. *J. Clin. Microbiol.* **48**, 2648–2650 (2010).
31. Colombo, A.P. *et al.* Impact of periodontal therapy on the subgingival microbiota of severe periodontitis: comparison between good responders and individuals with refractory periodontitis using the human oral microbe identification microarray. *J. Periodontol.* **83**, 1279–1287 (2012).
32. Hilty, M. *et al.* Disordered microbial communities in asthmatic airways. *PLoS One* **5**, e8578 (2010).
33. Park, H., Shin, J.W., Park, S. & Kim, W. Microbial communities in the upper respiratory tract of patients with asthma and chronic obstructive pulmonary disease. *PLoS One* **9**, e109710 (2014).
34. Rashid, T. & Ebringer, A. Autoimmunity in rheumatic diseases is induced by microbial infections via crossreactivity or molecular mimicry. *Autoimmune Dis.* **2012**, 539282 (2012).
35. van Heemst, J. *et al.* Crossreactivity to vinculin and microbes provides a molecular basis for HLA-based protection against rheumatoid arthritis. *Nat. Commun.* **6**, 6681 (2015).
36. van der Helm-van Mil, A.H. Risk estimation in rheumatoid arthritis: from bench to bedside. *Nat. Rev. Rheumatol.* **10**, 171–180 (2014).
37. Chen, L., Xiong, Z., Sun, L., Yang, J. & Jin, Q. VFDB 2012 update: toward the genetic diversity and molecular evolution of bacterial virulence factors. *Nucleic Acids Res.* **40**, D641–D645 (2012).
38. Goldbach-Mansky, R. *et al.* Comparison of *Tripterygium wilfordii* Hook F versus sulfasalazine in the treatment of rheumatoid arthritis: a randomized trial. *Ann. Intern. Med.* **151**, 229–240 W49–W51 (2009).
39. Tao, X., Younger, J., Fan, F.Z., Wang, B. & Lipsky, P.E. Benefit of an extract of *Tripterygium wilfordii* Hook F in patients with rheumatoid arthritis: a double-blind, placebo-controlled study. *Arthritis Rheum.* **46**, 1735–1743 (2002).
40. Lv, Q.-W. *et al.* Comparison of *Tripterygium wilfordii* Hook F with methotrexate in the treatment of active rheumatoid arthritis (TRIFRA): a randomised, controlled clinical trial. *Ann. Rheum. Dis.* **74**, 1078–1086 (2015).

ONLINE METHODS

Study cohort. RA was diagnosed at Peking Union Medical College Hospital on the basis of the 2010 American College of Rheumatology and EULAR classification criteria. All phenotypic information was collected upon a subject's initial visit to the hospital according to standard procedures. Individuals with RA between 18 and 65 years old with a disease duration of at least 6 weeks, at least one swollen joint and at least three tender joints were enlisted. Individuals were excluded if they had a history of chronic serious infection, any current infection or any type of cancer. Pregnant or lactating women were excluded. All individuals were informed of the risk of infertility associated with the treatment, and individuals with a desire to have children were excluded. Even though some of the individuals had experienced symptoms of RA for years, they were all DMARD naive because they had not been diagnosed with RA at local hospitals before visiting Peking Union Medical College Hospital, and they had taken only painkillers to relieve their symptoms.

The healthy control group had to meet the following inclusion criteria: 18–65 years of age, with normal values on recent screens for liver and kidney function, routine blood tests, erythrocyte sedimentation rate, fasting blood glucose, blood lipids, and blood pressure. Subjects were excluded if they had a history of chronic serious infection, any current infection, any type of cancer or autoimmune disease. Pregnant or lactating women were excluded. Subjects who had received antibiotic treatment within 1 month before participating in this study were also excluded. Informed consent was obtained from all subjects.

No formal power analysis was done for sample-size calculation. The sample size was no smaller than those used in previous MGWAS studies on other diseases^{20,41}.

The treatment was performed with MTX-based DMARDs as part of a single-blind randomized trial⁴⁰. 97% of the patients received MTX alone (7.5 mg weekly (QW) initially, increased to 15 mg (maximum of 0.3 mg/kg) QW from week 4 on; supplemented with 10 mg QW folate), T2 alone (20 mg TID), or MTX + T2 (same doses as when administered individually) (**Supplementary Table 1**). Other drugs used on the remaining patients included leflunomide, prednisolone, hydroxychloroquine and etanercept, which were not compared because of the small sample size (**Supplementary Table 1**). Reduction in DAS28-ESR after treatment was classified as good, moderate or no improvement according to the EULAR response criteria. As patients from all over China came to visit Peking Union Medical College Hospital, samples were not available from all patients after treatment.

The study was approved by the institutional review boards at Peking Union Medical College Hospital and BGI-Shenzhen.

Sample collection. Fecal samples were collected at Peking Union Medical College Hospital, transported frozen, and extracted at BGI-Shenzhen as previously described²⁰. Dental plaques were scraped from dental surfaces using ophthalmology forceps until a 3- μ l volume was obtained. Each dental sample was transferred into 200 μ l of 1 \times lysis buffer containing 10 mM Tris, 1 mM EDTA, 0.5% Tween 20 and 200 μ g/ml proteinase K (Fermentas) and incubated for 2 h at 55 °C. Lysis was terminated by incubation at 95 °C for 10 min, and the samples were then frozen at –80 °C until transport. DNA extraction was done according to the protocol for fecal samples. For saliva, 100 μ l of saliva was added to 100 μ l of 2 \times lysis buffer. The posterior pharynx wall was swabbed, and the swab was added to the tube containing saliva and buffer. The samples were then lysed and extracted in the same manner as the dental samples. All available samples were analyzed (**Supplementary Tables 1 and 2**). Fecal samples were missing or unusable for some subjects because of patient constipation or inappropriate sample preservation, and some of the oral samples could not be used because of a low concentration of microbial DNA.

Metagenomic sequencing and assembly. Paired-end metagenomic sequencing was done on the Illumina platform (insert size, 350 bp; read length, 100 bp), and the sequencing reads were quality controlled and *de novo* assembled into contigs with SOAPdenovo v2.04 (ref. 42) as described previously²⁰. The average rates of host contamination were 0.37% for fecal samples, 5.55% for dental samples and 40.85% for saliva samples.

Gene catalog construction. Gene prediction from the assembled contigs was done with GeneMark v2.7d. Redundant genes were removed using BLAT⁴³,

with a cutoff of 90% overlap and 95% identity (no gaps allowed), resulting in a non-redundant gene catalog of 3,800,011 genes for 212 fecal samples (including 21 of the DMARD-treated samples) and a catalog of 3,234,997 genes for the 203 treatment-naive oral samples (**Supplementary Tables 1 and 2**). The gene catalog for fecal samples was further integrated into an existing gut microbial reference catalog of 4.3 million genes using BLAT (95% identity, 90% overlap)²⁰, resulting in a final catalog of 5.9 million genes (from 481 samples). We determined relative abundances of the genes by aligning high-quality sequencing reads to the gut or oral reference gene catalog using the same procedure as in ref. 20.

Taxonomic annotation and abundance calculation. Taxonomic assignment of the predicted genes was done according to the Integrated Microbial Genomes (IMG, v400) database using an in-house pipeline detailed previously²⁰, with 70% overlap and 65% identity for assignment to phylum, 85% identity to genus, and 95% identity to species. The relative abundance of a taxon was calculated from the relative abundance of its genes.

α -Diversity and gene count. α -Diversity (within-sample diversity) was calculated on the basis of the gene profile of each sample according to the Shannon index, as described previously²⁰. The total gene count in each fecal sample was surveyed as in ref. 44. Genes with at least one mapped read were considered present.

PERMANOVA of the influence of clinical and lifestyle factors. Permutational multivariate analysis of variance (PERMANOVA)⁴⁵ was performed on the gene-abundance profiles of the samples to assess the effect of each of the factors listed⁴¹. We used Bray-Curtis distance and 9,999 permutations in R (3.10, vegan package⁴⁶).

Metagenome-wide association study (MGWAS). For case-control comparison of the fecal microbiome, we removed genes detected in less than 10% of the samples, leading to a set of 2,007,643 genes. 117,219 genes showed differences in relative abundance between controls and RA subjects (Wilcoxon rank-sum test, FDR < 0.3). These marker genes were then clustered into MLGs according to their abundance variation across all samples²⁰. For the construction of dental MLGs, 371,990 marker genes (Wilcoxon rank-sum test, FDR < 0.1) were selected from 1,900,774 genes (present in at least 10% of the samples). For salivary MLGs, we selected 258,055 marker genes (Wilcoxon rank-sum test, FDR < 0.1) from 2,030,636 genes (present in at least 10% of the samples).

Taxonomic assignment and abundance profiling of the MLGs were done according to the taxonomy and the relative abundance of the constituent genes, as previously described²⁰. Briefly, assignment to a species required that more than 90% of the genes in an MLG align with the species' genome with more than 95% identity and 70% overlap between the subject sequence and the query sequence. For an MLG to be assigned to a genus, more than 80% of its genes had to align with a genome with 85% identity in both DNA and protein sequences. Average identity with the genome(s) calculated from all genes was shown for reference only.

MLGs were further clustered according to Spearman's correlation between their abundances in all samples regardless of case-control status, and the co-occurrence network was visualized with Cytoscape 3.0.2. Correlation of MLGs from different body sites was analyzed in the same manner for the 69 subjects (36 controls and 33 treatment-naive RA subjects) who had provided a full set of fecal, dental and salivary samples.

Canonical correspondence analysis (CCA). CCA was performed on the MLG abundance profiles of control and RA samples to assess the effect of each of the factors listed⁴¹. The plot was generated by R (3.0.1, vegan package⁴⁶).

Association between MLGs and clinical indices. Spearman's correlation was assessed between the relative abundance of each MLG and continuous variables measured clinically, as previously described^{41,47}.

MLG-based classifier. Tenfold cross-validation was performed on a random forest model (R 3.0.1, randomForest4.6-10 package) using the MLG abundance profiles of the control and RA samples. The cross-validated error curves

(average of ten test sets each) from five trials of tenfold cross-validation were averaged, and the minimum error in the averaged curve plus the s.d. at that point were used as the cutoff. All sets (≤ 50) of MLG markers with an error less than the cutoff were listed, and the set with the fewest MLGs was chosen as the optimal set. The model was further applied to the related case-control pairs and samples from DMARD-treated subjects. Regression for the clinical indices and prediction of improvement after DMARD therapy were done in the same manner.

KEGG analysis. Putative amino acid sequences were translated from the gene catalogs and aligned against the proteins or domains in the KEGG databases (release 59.0, with animal and plant genes removed) using BLASTP (v2.2.24, default parameter, except $-e1e-5a6-b50-FFm8$). Each protein was assigned to a KEGG orthology group on the basis of the highest scoring annotated hit(s) containing at least one high-scoring segment pair scoring over 60 bits. KEGG orthology groups present in fewer than six fecal, dental or salivary samples were removed.

Identification of microbial proteins that possibly mimic human proteins. Sequences for human proteins mentioned in ref. 34 were downloaded from the NCBI protein database (HLA-DRB1*0401, HLA-B27 and collagen XI), and exact matches in five or six amino acid mimicry motifs were identified in the gut microbial reference gene catalog. Taxonomic and functional annotations of the genes were retrieved from our gut microbial reference gene catalog.

Statistical analyses of differentially enriched markers. Significant differences in the relative abundance of an MLG between individuals with RA and healthy

controls were identified by two-tailed Wilcoxon rank-sum test with $P < 0.05$. Enrichment in RA subjects or controls was then determined according to the higher rank-sum.

Differentially enriched KEGG modules were identified according to their reporter score^{24,41,48}, from the Z-scores of individual KEGG orthology groups. A reporter score of $Z = 1.6$ or higher (90% confidence according to a normal distribution) was used as a detection threshold for significantly differentiating modules.

41. Feng, Q. *et al.* Gut microbiome development along the colorectal adenoma-carcinoma sequence. *Nat. Commun.* **6**, 6528 (2015).
42. Luo, R. *et al.* SOAPdenovo2: an empirically improved memory-efficient short-read de novo assembler. *Gigascience* **1**, 18 (2012).
43. Kent, W.J. BLAT—the BLAST-like alignment tool. *Genome Res.* **12**, 656–664 (2002).
44. Le Chatelier, E. *et al.* Richness of human gut microbiome correlates with metabolic markers. *Nature* **500**, 541–546 (2013).
45. McArdle, B.H. & Anderson, M.J. Fitting multivariate models to community data: a comment on distance-based redundancy analysis. *Ecology* **82**, 290–297 (2001).
46. Zapala, M.A. & Schork, N.J. Multivariate regression analysis of distance matrices for testing associations between gene expression patterns and related variables. *Proc. Natl. Acad. Sci. USA* **103**, 19430–19435 (2006).
47. Karlsson, F.H. *et al.* Gut metagenome in European women with normal, impaired and diabetic glucose control. *Nature* **498**, 99–103 (2013).
48. Patil, K.R. & Nielsen, J. Uncovering transcriptional regulation of metabolism by using metabolic network topology. *Proc. Natl. Acad. Sci. USA* **102**, 2685–2689 (2005).